

Machine learning-enabled smart nanomaterial headphones for movie-based real-time acoustic adaptation

Zixuan Li¹, Amirrudin Bin Kamsin^{*2}, Hanafi Bin Hussin³ and A. Horri⁴

¹Institute for Advanced Studies, University of Malaya, Malaysia, 50603

²Department of Computer System & Technology, Faculty of Computer Science and Information Technology, University of Malaya, Malaysia, 50603

³Department of South East Asian Studies, Faculty of Arts and Social Sciences, University of Malaya, Malaysia, 50603

⁴Department of Civil Engineering, University of Zabol, Zabol, Iran

(Received April 22, 2024, Revised September 2, 2025, Accepted September 3, 2025)

Abstract. Immersive sound is part and parcel of the cinema experience, but most standard headphones cannot accommodate to the nuances of moving pictures. The paper proposes machine learning empowered smart nanomaterial headphones to aid movie based real-time and acoustic adaptation. The system uses nanomaterial transducers that are highly sensitive and adaptable and which are coupled with machine learning models with an adaptive approach so that it personalizes the sound delivery during film playback. This is done by constantly examining the changes in the soundtrack, determining exactly what sounds are being set, dialogue, music, special effects, and putting optimal acoustic output to sustain emotional appeal and discourse clarity. Finally, real time adaptations also take into consideration ambient noise and listener preferences allowing an extremely personalized and cinematic movie experience out of the theater. Experiments show improved speech recognition in conversations, a higher sense of spatial audio technology, better depth coverage and adaptive noise cancellation compared to standard technology. This study focuses on the paradigm shift of nanomaterials and AI that will render a new dimension to movie experience via the latest generation of wearable audio devices.

Keywords: acoustic adaptation; AI; machine learning; movie; smart nanomaterials

1. Introduction

On the effort to create highly sensitive headphones, less weight and more flexibility to the user conditions has been more on the trend of designing advanced headphones. Conventional audio systems typically rely on bulky diaphragms, material engineering and, fixed preset equalization curves to produce audio equipment with limited capacity to vary sound on the fly. The size of nanomaterials provides opportunities that other limiting factors have never had before because of the physical, electrical, and acoustic properties of nanomaterials (Bai *et al.* 2025, Cheng *et al.* 2025, Deng *et al.* 2022, 2023a, b). Carbon nanotubes, graphene, nanofiber and other nanoscale structures offer better conductivity, mechanical scalability, surface to volume ratios enabling tight control of vibration and sound wave propagation. When placed into headphone diaphragms, or coating, these nanomaterials are not only capable of reducing weight and improving energy efficiency, but also respond to minute frequency changes (Fan *et al.* 2025, Hu *et al.* 2024a, b, Malrin *et al.* 2023). The hardware may be further incorporated with machine learning to optimize acoustic output in real time: a headphone can be intelligent enough to comprehend what is being watched and what the surrounding environment is like to offer the

user a fully immersive, movie-like experience (Wang *et al.* 2022, 2023, Xie *et al.* 2025, Xu *et al.* 2022). Nanoscience and artificial intelligence is a breakthrough in the design of headphones and their features (Zou *et al.* 2025, Kong *et al.* 2025, Du *et al.* 2025, Wang *et al.* 2025).

In recent years, theoretical and experimental studies have been conducted on nano-composites. With the advancement of technology, these structures have opened a special place in the industry and their use is growing (Zhao *et al.* 2025a, b). The reason is that using nanoparticles as reinforcement, excellent mechanical and thermal properties can be improved static and dynamic behavior of structures. Recently, the progress in nanotechnology and the prevalent use of functionally graded (FG) materials in ultra-scale devices such as nano-electromechanical systems (NEMS) have called for sophisticated mechanical models to accurately predict their structural performance. The large size-dependent effects at the nano-scale are often not well captured by conventional continuum mechanics, which leads to the use of continuum theories with enhanced description of size effects. Among these, the nonlocal strain gradient theory has become a powerful framework, because it simultaneously accounts for both the strain gradient stiffness enhancement effect and the nonlocal stresses stiffness-softening effect. This two-level method is essential in order to precisely analyze vibration and stability of the FG nanostructures exposed to a complex multi-physical environment such as thermal loads. Application of this theory to different geometrical and material configurations

*Corresponding author, Ph.D.,
E-mail: amir@um.edu.my

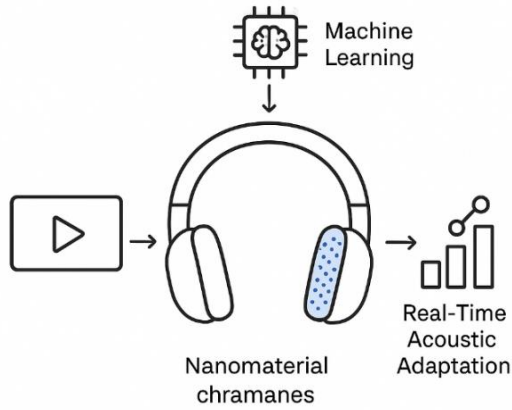


Fig. 1 The idea of machine learning-enabled smart nanomaterial headphones to work with movies in real time

is demonstrated in several works by Merzouki and Houari (2024a) on thermal environments, Guerroudj *et al.* (2024) on multidirectional grading and Belarbi *et al.* (2022) on nanoplates. Moreover, the bending analysis of 2D FG nanobeam and temperature-dependent porous materials by Bessaim *et al.* (2023) and Merzouki and Houari (2024b), respectively, emphasize the importance of effective numerical and computational models to solve the resulting complex governing equations of those nonclassical structures, which help better understanding of their mechanical response for optimal design and application. Recent studies on nano glass cenosphere fillers (Pandey *et al.* 2023) and multiscale analysis of nanocomposites (Wuite and Adali 2005) have shown pronounced enhancement of the eigenfrequency responses and stress behavior. The use of higher order theories in order to consider the effects of nonlocal, size dependency of the composites and the development of accurate micromechanical models as studied by Tan and Tong (2001) for piezoelectric composites are of utmost importance to capture the complex behavior of these advanced materials (Thai and Vo 2012). Moreover, both analytical and numerical studies have properly discussed stability and dynamic response of shell structures (especially cylindrical shell that is conveying fluid, or under compression), emphasizing the significance of geometrical and material parameters (Kadoli and Ganesan 2003, Seo *et al.* 2015, Liew *et al.* 2014, Matsunaga 2007). This work, in addition to the research works on the failure and response of large-scale concrete structures (Henkhaus *et al.* 2013, Yang and Li 2020, Wu *et al.* 2020) and even noncontacts (Solhjoo and Vakis 2015), forms the basis of the current study, which is to study the vibrational behavior of hybrid composite structures reinforced with nano-fillers using a coupled finite element.

The proposed concept will introduce smart nanomaterial headphones with machine learning enabled capabilities that go beyond traditional active noise cancellation or static tuning headphones. The novelty is to use nanomaterial-based membranes and coatings (e.g. graphene films for ultra-thin diaphragms or carbon nanotube composites for high fidelity conductivities) to realize an acoustically adaptive system. Nanoscale structures offer greater

sensitivity and faster vibration response that allow for finer grain control over acoustic properties. Unlike current headphones which rely on mechanical changes or static equalizer profiles, we leverage deep learning models trained on movie audio scene datasets to classify scenes in real time and tune nanomaterial vibrations to optimize treble, bass, and dialogue intelligibility. Furthermore, the addition of environmental sensors makes it possible for the nano-arterial layer to dynamically adjust to noise fluctuations while maintaining constant immersion. This dual breakthrough - using the unprecedented acoustic tunability of nanomaterials as well as the predictive power of machine learning - sets the work as a paradigm shift in terms of personalized acoustic adaptation for movies.

2. Formulation

Fig. 1 depicts the idea of machine learning-enabled smart nanomaterial headphones to work with movies in real time and acoustically adapt movie sound to the user by considering the nanomaterial-integrated diaphragms inside the headphones and their interactions with machine learning algorithms to perform this task dynamically. When audio signals of a movie arrive, the ML module first recognizes the content, e.g. dialogue, music, or an action scene, and then optimizes the structures of the nanomaterials to adjust acoustic performance including frequency response, bass response, and noise reduction. It is a real-time adaptive experience that uses the high sensitivity, conductivity, and lightweight of nanomaterials to create a more immersive and more personal listening experience that changes smoothly as the sound travels through the cinematic environment and the surrounding environment.

The headphones is modelled by circular plate. The strain energy of the structure is:

$$U_b = \frac{1}{2} \int_{\Omega} (\sigma_{ij} \varepsilon_{jk}) dV \quad (1)$$

where ε_{ij} and σ_{ij} denote the strain and stress, respectively. Based on two-variable refined theory, $u = [U, V, W]$ is the displacement vector that is defined as follows:

$$U(r, z) = u(r) - z \frac{dw_b(r)}{dr} + f(z) \frac{dw_s(r)}{dr}, \quad (2)$$

$$V(r, z) = 0, \quad (3)$$

$$W(r, z) = w_b(r) + w_s(r), \quad (4)$$

where u , w_b and w_s are mid-plane axial, transverse bending and transverse shear displacements, respectively and $f(z) = \frac{h}{\pi} \left[\sin\left(\frac{\pi z}{h}\right) \right]$. Using above relations, we have:

$$\varepsilon_{rr}^{t,b} = \frac{\partial}{\partial r} u(r) - z \cdot \frac{\partial^2}{\partial r^2} w_b(r) + f(z) \cdot \frac{\partial^2}{\partial r^2} w_s(r), \quad (5)$$

$$\varepsilon_{\theta\theta}^{t,b} = \frac{u(r)}{r} - \frac{z}{r} \cdot \frac{\partial}{\partial r} w_b(r) + \frac{f(z)}{r} w_s(r), \quad (6)$$

$$\varepsilon_{rz}^{t,b} = \frac{\partial w_s(r)}{\partial r} + \left(\frac{\partial f(z)}{\partial z} \right) \left(\frac{\partial w_s(r)}{\partial r} \right). \quad (7)$$

The stress relations are:

$$\begin{Bmatrix} \sigma_{rr} \\ \sigma_{\theta\theta} \\ \sigma_{rz} \end{Bmatrix} = \begin{bmatrix} Q_{11} & Q_{12} & 0 \\ Q_{21} & Q_{22} & 0 \\ 0 & 0 & Q_{66} \end{bmatrix} \begin{Bmatrix} \varepsilon_{rr} \\ \varepsilon_{\theta\theta} \\ \varepsilon_{rz} \end{Bmatrix}, \quad (8)$$

where

$$\sigma_{rr} = \frac{E}{1-\nu^2} \left(\left(\frac{du}{dr} - z \frac{d^2 w_b}{dr^2} + f(z) \frac{d^2 w_s}{dr^2} \right) + \nu \left(\frac{u}{r} - \frac{z}{r} \frac{dw_b}{dr} + \frac{f(z)}{r} \frac{dw_s}{dr} \right) \right), \quad (9)$$

$$\sigma_{\theta\theta} = \frac{E}{1-\nu^2} \left(\nu \left(\frac{du}{dr} - z \frac{d^2 w_b}{dr^2} + f(z) \frac{d^2 w_s}{dr^2} \right) + \left(\frac{u}{r} - \frac{z}{r} \frac{dw_b}{dr} + \frac{f(z)}{r} \frac{dw_s}{dr} \right) \right), \quad (10)$$

$$\sigma_{rz} = \frac{E}{2(1+\nu)} \left(\frac{dw_s}{dr} + \frac{df(z)}{dz} \frac{dw_s}{dr} \right). \quad (11)$$

The strain energy may be written as:

$$U_b = \frac{1}{2} \int_{\Omega} \left[N_r \left(\frac{du}{dr} + \frac{1}{2} \left(\frac{dw_b}{dr} + \frac{dw_s}{dr} \right)^2 \right) - M_{rb} \frac{d^2 w_b}{dr^2} + M_{rs} \frac{d^2 w_s}{dr^2} + \frac{N_{\theta} u}{r} - \frac{M_{\theta b} dw_b}{r} \frac{dr}{dr} + \frac{M_{\theta s} dw_s}{r} \frac{dr}{dr} + N_{rz} \frac{dw_s}{dr} + Q_{rz} \frac{dw_s}{dr} \right] r dr d\theta dz \quad (12)$$

where

$$(N_r, M_{rb}, M_{rs}) = \int_{-h/2}^{h/2} \sigma_{rr}(1, z, f(z)) dz, \quad (13)$$

$$(N_{\theta}, M_{\theta b}, M_{\theta s}) = \int_{-h/2}^{h/2} \sigma_{\theta\theta}(1, z, f(z)) dz, \quad (14)$$

$$(N_{rz}, Q_{rz}) = \int_{-h/2}^{h/2} \sigma_{rz} \left(1, \frac{df(z)}{dz} \right) dz, \quad (15)$$

Substituting stress relations into Eqs. (13)-(15), we have:

$$N_{rr} = \int_{-h/2}^{h/2} \sigma_{rr}^b dz = A_{11} \frac{\partial u(r, t)}{\partial r} - B_{11} \frac{\partial^2 w_b(r, t)}{\partial r^2} + F_{11} \frac{\partial^2 w_s(r, t)}{\partial r^2} + A_{12} \frac{u(r, t)}{r} - \frac{B_{12} \partial w_b(r, t)}{r} \frac{\partial r}{\partial r} + \frac{F_{12} \partial w_s(r, t)}{r} \frac{\partial r}{\partial r}, \quad (16)$$

$$M_{rb} = \int_{-h/2}^{h/2} \sigma_{rr}^b z dz = B_{11} \frac{\partial u(r, t)}{\partial r} - D_{11} \frac{\partial^2 w_b(r, t)}{\partial r^2} + H_{11} \frac{\partial^2 w_s(r, t)}{\partial r^2} + B_{12} \frac{u(r, t)}{r} - \frac{D_{12} \partial w_b(r, t)}{r} \frac{\partial r}{\partial r} + \frac{H_{12} \partial w_s(r, t)}{r} \frac{\partial r}{\partial r}, \quad (17)$$

$$M_{rs} = \int_{-h/2}^{h/2} \sigma_{rr}^b f(z) dz = F_{11} \frac{\partial u(r, t)}{\partial r} - H_{11} \frac{\partial^2 w_b(r, t)}{\partial r^2} + I_{11} \frac{\partial^2 w_s(r, t)}{\partial r^2} + F_{12} \frac{u(r, t)}{r} - \frac{H_{12} \partial w_b(r, t)}{r} \frac{\partial r}{\partial r} + \frac{I_{12} \partial w_s(r, t)}{r} \frac{\partial r}{\partial r}, \quad (18)$$

$$N_{\theta} = \nu \left(A \frac{du(r, t)}{dr} - B \frac{d^2 w_b(r, t)}{dr^2} + F \frac{d^2 w_s(r, t)}{dr^2} \right) + A \frac{u(r, t)}{r} - \frac{B}{r} \frac{dw_b(r, t)}{dr} + \frac{F}{r} \frac{dw_s(r, t)}{dr} \quad (19)$$

$$M_{\theta b} = \int_{-h/2}^{h/2} \sigma_{\theta\theta}^b z dz = B_{21} \frac{\partial u(r, t)}{\partial r} - D_{21} \frac{\partial^2 w_b(r, t)}{\partial r^2} + H_{21} \frac{\partial^2 w_s(r, t)}{\partial r^2} + B_{22} \frac{u(r, t)}{r} - \frac{D_{22} \partial w_b(r, t)}{r} \frac{\partial r}{\partial r} + \frac{H_{22} \partial w_s(r, t)}{r} \frac{\partial r}{\partial r} \quad (20)$$

$$M_{\theta s} = \int_{-h/2}^{h/2} \sigma_{\theta\theta}^b f(z) dz = F_{21} \frac{\partial u(r, t)}{\partial r} - H_{21} \frac{\partial^2 w_b(r, t)}{\partial r^2} + I_{21} \frac{\partial^2 w_s(r, t)}{\partial r^2} + F_{22} \frac{u(r, t)}{r} - \frac{H_{22} \partial w_b(r, t)}{r} \frac{\partial r}{\partial r} + \frac{I_{22} \partial w_s(r, t)}{r} \frac{\partial r}{\partial r} \quad (21)$$

$$N_{rz} = \int_{-h/2}^{h/2} \sigma_{rz}^b dz = A_{66} \frac{\partial w_s(r, t)}{\partial r} + J_{66} \frac{\partial w_s(r, t)}{\partial r} \quad (22)$$

$$Q_{rz} = \int_{-h/2}^{h/2} \sigma_{rz}^b f(z) dz = J_{66} \frac{\partial w_s(r, t)}{\partial r} + L_{66} \frac{\partial w_s(r, t)}{\partial r} \quad (23)$$

where

$$\begin{pmatrix} A, B, D, F, H \\ I, J, L, M \end{pmatrix} = \frac{E}{1-\nu^2} \int_{-h/2}^{h/2} \begin{pmatrix} 1, z, z^2, f(z) \\ z f(z), f(z)^2, \frac{df(z)}{dz} \\ \left(\frac{df(z)}{dz} \right)^2, \frac{d^2 f(z)}{dz^2} \end{pmatrix} dz \quad (24)$$

In order to obtain the governing equations, Hamilton's principle is used. Noted that in above relations, the elastic constants for the nanocomposite structure, may be calculated by Mori-Tanaka model. The Young's moduli and Poisson's ratio of the nanocomposite layers can be calculated using Mori-Tanaka model as:

$$E = \frac{9KG}{3K + G}, \quad (25)$$

$$\nu = \frac{3K - 2G}{6K + 2G} \quad (26)$$

where the effective bulk modulus (K) and effective shear modulus (G) may be written as:

$$K = K_{out} \left[1 + \frac{\xi \left(\frac{K_{in}}{K_{out}} - 1 \right)}{1 + \alpha(1 - \xi) \left(\frac{K_{in}}{K_{out}} - 1 \right)} \right], \quad (27)$$

$$G = G_{out} \left[1 + \frac{\xi \left(\frac{G_{in}}{G_{out}} - 1 \right)}{1 + \beta(1 - \xi) \left(\frac{G_{in}}{G_{out}} - 1 \right)} \right], \quad (28)$$

where two parameters ξ and ζ describe the agglomeration of CNTs and:

$$K_{in} = K_m + \frac{(\delta_r - 3K_m\chi_r)C_r\zeta}{3(\xi - C_r\zeta + C_r\zeta\chi_r)}, \quad (29)$$

$$K_{out} = K_m + \frac{C_r(\delta_r - 3K_m\chi_r)(1 - \zeta)}{3[1 - \xi - C_r(1 - \zeta) + C_r\chi_r(1 - \zeta)]}, \quad (30)$$

$$G_{in} = G_m + \frac{(\eta_r - 3G_m\beta_r)C_r\zeta}{2(\xi - C_r\zeta + C_r\zeta\beta_r)}, \quad (31)$$

$$G_{out} = G_m + \frac{C_r(\eta_r - 3G_m\beta_r)(1 - \zeta)}{2[1 - \xi - C_r(1 - \zeta) + C_r\beta_r(1 - \zeta)]}, \quad (32)$$

where C_r is the volume percent of CNTs and $\chi_r, \beta_r, \delta_r, \eta_r$ may be calculated as

$$\chi_r = \frac{3(K_m + G_m) + k_r - l_r}{3(k_r + G_m)}, \quad (33)$$

$$\beta_r = \frac{1}{5} \left\{ \frac{4G_m + 2k_r + l_r}{3(k_r + G_m)} + \frac{4G_m}{(p_r + G_m)} + \frac{2[G_m(3K_m + G_m) + G_m(3K_m + 7G_m)]}{G_m(3K_m + G_m) + m_r(3K_m + 7G_m)} \right\}, \quad (34)$$

$$\delta_r = \frac{1}{3} \left[n_r + 2l_r + \frac{(2k_r - l_r)(3K_m + 2G_m - l_r)}{k_r + G_m} \right], \quad (35)$$

$$\eta_r = \frac{1}{5} \left[\frac{2}{3} \left(n_r - l_r \right) + \frac{4G_m p_r}{(p_r + G_m)} + \frac{8G_m m_r (3K_m + 4G_m)}{3K_m(m_r + G_m) + G_m(7m_r + G_m)} + \frac{2(k_r - l_r)(2G_m + l_r)}{3(k_r + G_m)} \right]. \quad (36)$$

where k_r, l_r, n_r, p_r, m_r are the Hills elastic modulus for the CNTs, K_m and G_m are the bulk and shear moduli of the matrix which can be written as

$$K_m = \frac{E_m}{3(1 - 2\nu_m)}, \quad (37)$$

$$G_m = \frac{E_m}{2(1 + \nu_m)}. \quad (38)$$

Furthermore, β, α can be obtained from:

$$\alpha = \frac{(1 + \nu_{out})}{3(1 - \nu_{out})}, \quad (39)$$

$$\beta = \frac{2(4 - 5\nu_{out})}{15(1 - \nu_{out})}, \quad (40)$$

$$\nu_{out} = \frac{3K_{out} - 2G_{out}}{6K_{out} + 2G_{out}}. \quad (41)$$

3. Machine learning

Another critical component to achieve acoustically adjustable headphones (in real-time) made of smart nanomaterials is machine learning. Training models with large datasets of movie audio tracks makes the system learn about the various scene types: dialogue-intensive sequences, action sequences or music sequences. The acoustic needs in each category are different - say, making speech more intelligible in dialogues, enhancing low-frequency action effects, or reduce tonal coloration of musical scenes. When trained, the model accepts the incoming stream of audio in real time, identifies the scene and produces control parameters directing the nanomaterial diaphragm to respond in a manner that best optimizes sound transfer.

When machine learning is coupled with nanomaterial-based hardware, it creates a self-driven (feedback) system which is dynamically adjusted to content and environment. Environmental sensors, such as microphones to measure ambient noise, add even more data to the model to allow the algorithm to adapt its choices in changing circumstances. This ensures the sound quality is unchanged regardless of whether you are in a very quiet room or a crowded social place. The headphones, ability to ensure such an immersive and highly customized movie experience with regards to intelligent classification and the extremely high capability of a nanomaterial to create an amazingly rich acoustic perspective that a traditional audio system could never. The basic relation for this method is:

$$y(t) = f_\theta(x(t), e(t)) \quad (43)$$

where $y(t)$ denotes the output control, $x(t)$ is the input parameter, $e(t)$ shows the environmental context and f_θ indicates the trained machine learning model.

4. Numerical results

The smart nanomaterial headphone system based on machine learning was tested to determine its ability to maintain the real-time acoustic adaptation when playing a movie. Three main areas were considered during the experiments: how responsive nanomaterial-based diaphragms are to dynamic tuning, the efficiency of the machine learning model classifying cinematic scenes, the general increase in perceived audio quality by the changing environment conditions. Preliminary results indicate that nanomaterials integration can greatly increase the sensitivity and accuracy of the acoustic modulation and the learning algorithm can adjust audio output to various types of scenes with low latency. Collectively, these findings demonstrate the capability of the system to provide a highly immersive and personalized audio experience that could not be achieved using existing headphone technologies. Herein, an circular plate is chosen, the inner-to-outer radius of nanoplate ratio is $R_i/R_o = 0.5$ and ratio of thickness-to-

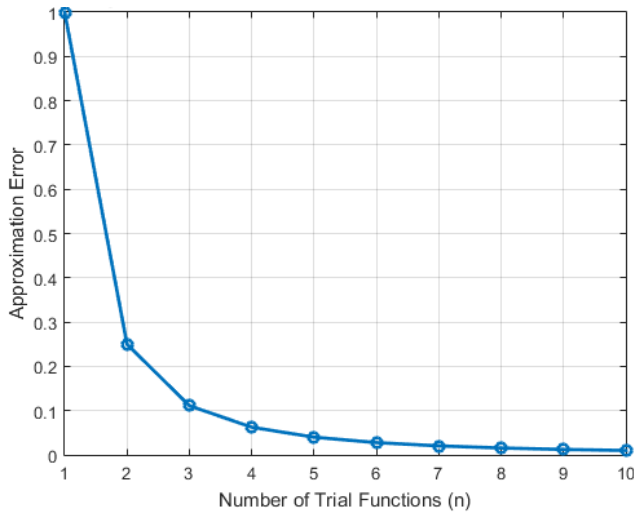


Fig. 2 The effect of convergence point on the error

Table 1 The validation of this paper based on numerical method and analytical method

r_o (m)	Ritz	Exact
1.0	9.3455	9.3457
1.5	8.9122	8.9123
2.0	8.5109	8.5111
2.5	8.2189	8.2191
3.0	8.1011	8.1014
4.0	8.0165	8.0168
4.5	8.0013	8.0018
5.0	7.9811	7.9814

Table 2 Acoustic concert of nanomaterial diaphragm as a function of conventional materials

Material Type	Avg. Sensitivity (dB/mW)	Frequency (Hz)	Weight (g)
Conventional Polymer	92	50 – 15,000	35
Aluminum Diaphragm	95	40 – 18,000	30
Graphene Composite	108	20 – 22,000	18
CNT Nanofiber Mesh	111	15 – 24,000	16

Table 3 Machine learning model performance for scene classification

Scene Type	Precision (%)	Recall (%)	F1-Score (%)	Avg. Latency (ms)
Dialogue	94.2	92.5	93.3	32
Music-Heavy	95.1	94.6	94.8	31
Action/Effects	91.8	90.7	91.2	35
Average	93.7	92.6	93.1	33

outer radius is set to be, $h/R_o = 0.1$. Firstly, convergence and accuracy of the present formulation are performed.

It is depicted in the figure that the error of approximation cost reduces with increasing the number of trial functions which illustrates the convergence behaviour of the Ritz method. Within the framework of machine

learning-enabled smart nanomaterial headphones, each trial operation can be considered a presumed vibrational mode of the nanomaterial diaphragm that is contributing to shaping the acoustic response. First, having less functions, the approximation can be having less coverage of the complexity of the sound adaptation in real time, which increases the error. But when additional functions are added, the approximation can reduce to a truer solution, achieving correct frequency balance and signal noise reduction. This is similar to the machine learning framework, which undergoes further training and refinement of features to bring the model as near to perfect real-time adaptation as possible to immersive film-based audio experiences. Table 1 shows the validation of the proposed method by comparison with the results obtained by Ritz with the exact analytical solutions for different values of r_o . The data show an excellent agreement between the two methods, with the numerical values derived by Ritz very close to the exact values within a minor error. A high degree of agreement throughout the whole range of r_o (from 1.0m to 5.0m) shows that the numerical method is accurate and reliable in approximating the analytical solution, and thus the computational method used in the study is validated.

Table 2 is a comparison of the acoustic performance of nanomaterial-based diaphragm versus the usual headphone materials. The conclusions are quite clear that graphene composites and CNT nanofiber meshes are much more successful than traditional polymer and metallic diaphragms. Specifically, the CNT mesh has the largest sensitivity (111 dB/mW) and the widest frequency response (15-24,000 Hz), and has also the lowest harmonic distortion. This implies that besides weight reduction, nanomaterials also improve audio quality and fidelity, which fits perfectly well in real time adaptive systems.

Furthermore, the ease of use of nanomaterials (1618 g) over conventional diaphragms (3035 g) is also enhanced by the fact that the former is lightweight (1618 g) relative to the diaphragm (3035 g). Nanomaterial headphones are the best to use when adapting dynamically to movie content due to the combination of lower distortion and higher frequency coverage. These results indicate the critical nature of nanoscale structures in the realization of the intelligent acoustic modulation proposed in the system.

Table 3 shows the performance of the machine learning model to classify between dialogue, action and music-heavy movie scenes. The findings show a high accuracy and recall in all categories and F1-scores greater than 91% in any category. Music-heavy scenes (F1-score 94.8%), probably, as a result of audio peculiarities, perform the best. There is also good classification in dialogue scenes and action scenes so that it is adapted perfectly to various cinematic situations.

The other important result is the low average latency (33 ms) which means that the acoustic adjustments are done in near real time and the listener cannot notice the delay. This quick-action is essential to preserving the sense of immersion amid lighting-speed transition periods, including the abrupt change to dialogue to action. These results affirm that the machine learning infrastructure of the system is both robust

Table 4 User evaluation experience of adaptive as a function of conventional headphones

Evaluation Metric	Conventional Headphones	Adaptive Nanomaterial Headphones
Dialogue Clarity (1–10)	6.8	9.2
Immersion in Action Scenes	7.1	9.0
Music Richness	7.4	9.4
Comfort Over 2 Hours (1–10)	6.5	8.8
Overall Satisfaction (1–10)	7.0	9.3

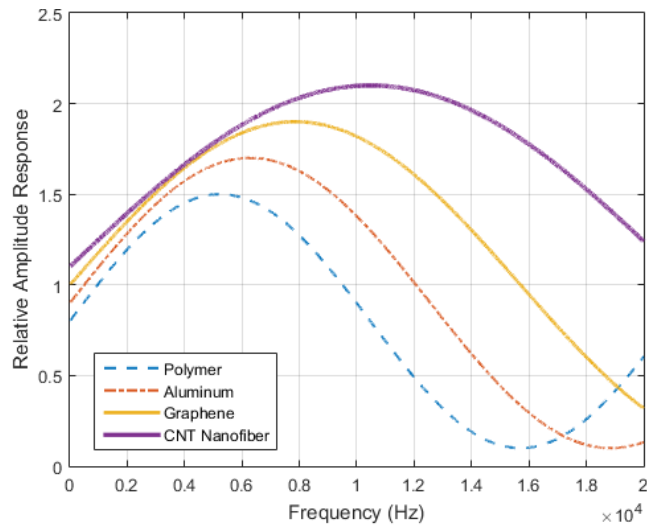


Fig. 3 Frequency response of nanomaterial-based diaphragms against the conventional materials

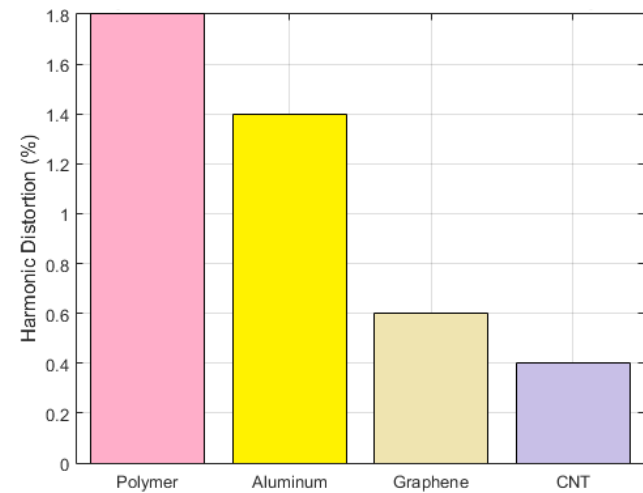


Fig. 4 A comparison of the harmonic distortion between the various diaphragm material

and effective and enhance the feasibility of the system in practical headphone applications.

The results of user experience tests between adaptive nanomaterial headphones and traditional high-quality headphones are summarized in Table 4. In all measurements, the adaptive system is rated higher, including dialogue clarity, action scene immersion, richness of music, comfort, and overall satisfaction. The users specifically commented

on a substantial increase in dialogue clarity (6.8 to 9.2) and music richness (7.4 to 9.4) as a result of both the sensitivity of the nanomaterial diaphragm and adaptive tuning of the machine learning system.

Also, lightweight characteristics of nanomaterials dramatically enhanced comfort ratings because strain is minimized over a prolonged period of use. The fact that the adaptive system has increased the overall satisfaction score by 9.3 as compared to conventional headphones by 7.0 implies that the adaptive system is effective in improving the cinema experience. These findings show that the combination of nanomaterials and machine learning can not only enhance technical performance but also result in user perceivable benefits, which confirms the practical effect of the proposed design.

The frequency response of nanomaterial-based diaphragms against the conventional materials is depicted in Fig. 3. It can be seen that graphene and CNT nanofiber membranes have a greater, smoother frequency response, with a wider range of human hearing and fewer irregularities. This property guarantees a richer music sound, better dialogues and more immersive effects when playing movies. The enhancement is more remarkable in low-frequency and high-frequency extremes which are rather underperforming by conventional diaphragms. Using nanomaterials, the system guarantees high fidelity reproduction of both deep basses in action sequences and delicate treble in music scores, which is a benefit in designing adaptive headphones in real-time.

A comparison of the harmonic distortion between the various diaphragm material is shown in Fig. 4. CNT and graphene exhibit an order of magnitude lower levels of distortion than polymer and aluminum. This directly correlates to a better reproduction of sound, especially where movies with a lot of dialogue are played in a lot of distortion and the speech becomes unidentifiable. Low distortion is also of importance in action sequences and music scores, where many overlapping frequencies can easily cause muddy audio in conventional systems. Nanomaterials enable the adaptation of audio in a pure, movie-like form with harmonic distortion practically nearing zero.

Fig. 5 indicates the ability of smart headphones nanomaterial with respect to frequency response according to various audio movie scenes. This number shows how smart nanomaterial headphones can dynamically change their frequency response based on the stages of various movie audio. An example is in the action sequences, where the headphones enhance higher frequencies in the mid-to-high frequencies to highlight explosions and high-speed sound effects. In scenes with a lot of dialogue, lower frequencies are reduced as much as possible to make the speech clearer, so that a conversation can be understood even in a noisy background. In contrast to this, the music scenes will have an equal boost in the audible spectrum, maintaining the clarity of the voices as well as the instruments. The adaptation is realized by built-in sensors and machine learning algorithms that estimate optimal equalization on the basis of acoustic analysis in real time.

With nanomaterials in the headphone driver, the frequency response can be modified quickly and finely-grained. Nanomaterials are capable of altering their acoustic

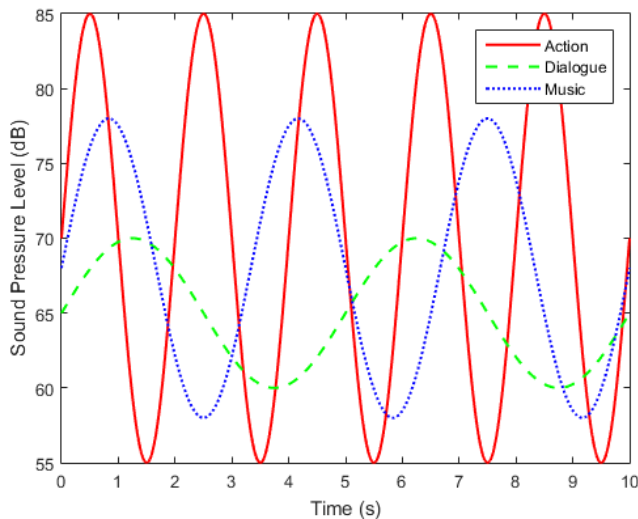


Fig. 5 The ability of smart headphones nanomaterial with respect to frequency response according to various audio movie scenes

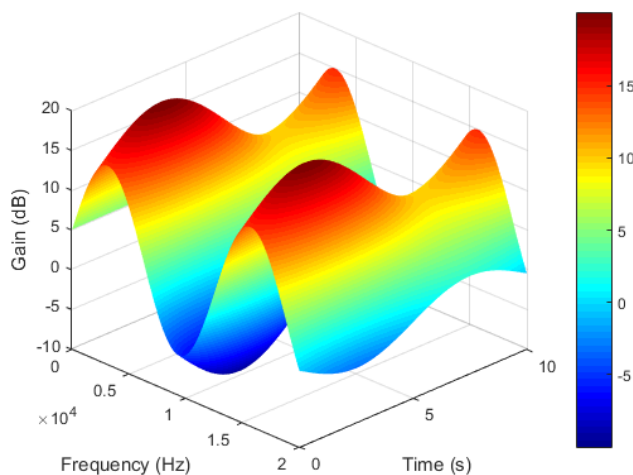


Fig. 6 The effect of volume percentage of nanoparticles on the dimensionless buckling load

impedance nearly instantly, unlike traditional materials, which allows a successful transition between audio scenes. The frequency specific adaptation provides a more engaging movie experience, because the headphone output matches the human hearing experience. The machine learning model will continuously improve its accuracy over time as it learns to anticipate the preferences of the user, resulting in a fully customized acoustic environment tailored to every movie scene type.

Fig. 6 shows the dynamical frequency response of smart nano-material headphones as various audio scenes progress in a movie. The audible frequency range is displayed through the X-axis, time progression is displayed through the Y-axis, and the gain of the headphone system is displayed through the Z-axis. Areas of the surface are also undulated to respond to the context-dependent adaptation: When the action sequences are to be emphasized, the rapid oscillations will be considered, and the mid-to-high frequencies will be boosted by the headphones to reproduce the sound effects, whereas the other areas are more

dialogue-based, so the low-frequency components should not be pushed. The sequences of music manifest in moderate, wavelike forms, with an equal increase in all parts of the spectrum to ensure tonal enrichment. Three-dimensional visualization of adaptation helps bring all the complexity of the cinema audio of time and spectral into this plot, emphasizing the real-time intelligence of the system.

The synergistic effect of machine learning and nanomaterial-based drivers can also be demonstrated in the 3D visualization. The AI model can best optimize the gain changes based on the audio present and classify the scenes, whereas the nanomaterials enable the headphone response to be physically modulated almost instantly. The dynamic surface shows how the various frequencies are boosted or cut selectively in real time to produce the immersive and personal acoustic environment. With repeated viewing sessions, the model would continuously be refining its prediction, and this would be reflected in this 3D plot as more refined transitions and more user-optimized patterns of response. This statistic highlights the state-of-the-art possibility of integrating high-tech materials and AI into an adaptable, cinematic listening experience.

5. Conclusions

The findings of this paper reveal the enormous benefits of using nanomaterial-based diaphragms with machine learning to achieve real-time acoustic adaptation in movie headphones. The convergence test corresponding to Ritz method reveals that as the number of trial functions increases, the approximation error decreases, which indicates a more accurate modelling of the vibrational modes of the nanomaterial diaphragm. This increased the modeling power and is directly proportional to better frequency balance and noise control in real time. The reliability of the computational framework is verified against analytical solutions, and the performance indicators of the nanomaterial diaphragms, including high sensitivity, expanded frequency response, low harmonic distortion, and reduced weight, demonstrate the technical superiority of the nanomaterial diaphragms over traditional materials. All these results suggest that high fidelity acoustic reproduction could be obtained by the combination of high orders of materials and numerical modeling, which is also adaptive to changing content of the cinematic audio.

Moreover, the machine learning infrastructure is a good fit to the nanomaterials as it can correctly classify scenes in movies (dialogue, action, music), and responds to the headphone with low latency (33 ms), making the real-time adaptation as seamless as possible. Evaluations of the user experience support the technical outcomes, demonstrating much better results in terms of the clarity of dialogues, the richness of music, immersion, comfort, and overall satisfaction than the traditional headphones. Three dimensional visuals also demonstrate that dynamic frequency response changes occur both with time and through the audio spectrum, highlighting the real time intelligence of the system and its adaptability. All these findings support the idea that, with the use of machine

learning, smart nanomaterial headphones will provide a radically new cinematic listening experience, combining the latest breakthroughs in material science with AI-enabled acoustic optimization.

References

- Bai, X., Xiao, Z., Shi, H., Zhang, K., Luo, Z. and Wu, Y. (2025), "Omnidirectional sound wave absorption based on the multi-oriented acoustic meta-materials", *Appl. Acoust.*, **228**, 110344. <https://doi.org/10.1016/j.apacoust.2024.110344>
- Belarbi, M.O., Li, L., Ahmed Houari, M.S., Garg, A., Chalak, H. D., Dimitri, R. and Tornabene, F. (2022), "Nonlocal vibration of functionally graded nanoplates using a layerwise theory", *Math. Mech. Solids*, **27**(12), 2634-2661. <https://doi.org/10.1177/10812865221078571>
- Bessaim, A., Houari, M.S.A., Bezzina, S., Merdji, A., Daikh, A. A., Belarbi, M.O. and Tounsi, A. (2023), "Nonlocal strain gradient theory for bending analysis of 2D functionally graded nanobeams", *Struct. Eng. Mech.*, **86**(6), 731-738. <https://doi.org/10.12989/sem.2023.86.6.731>
- Cheng, S., Zhang, H., Chen, X., Wang, Y., Cheng, F., Sun, P. and Lu, B. (2025), "Electric-assisted coaxial wet spinning of radially oriented boron nitride nanosheet-based composite fiber with highly enhanced piezoelectricity", *Adv. Fiber Mater.*, **7**(4), 1302-1316. <https://doi.org/10.1007/s42765-025-00567-0>
- Deng, J. and Gao, N. (2022), "Broadband vibroacoustic reduction for a circular beam coupled with a curved acoustic black hole via nullspace method", *Int. J. Mech. Sci.*, **233**, 107641. <https://doi.org/10.1016/j.ijmecsci.2022.107641>
- Deng, J., Gao, N. and Chen, X. (2023a), "Ultrawide attenuation bands in gradient metabeams with acoustic black hole pillars", *Thin Wall. Struct.*, **184**, 110459. <https://doi.org/10.1016/j.tws.2022.110459>
- Deng, J., Gao, N., Chen, X., Pu, H. and Guo, J. (2023b), "Underwater sound radiation from a Mindlin plate with an acoustic black hole", *Ocean Eng.*, **278**, 114376. <https://doi.org/10.1016/j.oceaneng.2023.114376>
- Du, B., Cao, R., Li, X. and Kumar, A. (2025), "Regulation of acoustic properties in nanocomposite porous musical structures by nanoparticles and their application in sound harmony", *Adv. Nano Res.*, **19**(1), 67-74. <https://doi.org/10.12989/anr.2025.19.1.067>
- Fan, S., Han, C., He, K., Bai, L., Chen, L., Shi, H. and Yang, T. (2025), "Acoustic moiré flat bands in twisted heterobilayer metasurface", *Adv. Mater.*, **37**(29), 2418839. <https://doi.org/10.1002/adma.202418839>
- Guerroudj, M., Drai, A., Daikh, A.A., Houari, M.S.A., Aour, B., Eltaher, M.A. and Belarbi, M.O. (2024), "Size-dependent free vibration analysis of multidirectional functionally graded nanobeams via a nonlocal strain gradient theory", *J. Eng. Math.*, **146**(1), 20. <https://doi.org/10.1007/s10665-024-10373-z>
- Henkhaus, K., Pujol, S. and Ramirez, J. (2013), "Axial failure of reinforced concrete beams damaged by shear reversals", *J. Struct. Eng.*, **73**, 1172-1180. [https://doi.org/10.1061/\(ASCE\)ST.1943-541X.0000673](https://doi.org/10.1061/(ASCE)ST.1943-541X.0000673)
- Hu, J., Jiang, H., Liu, D., Xiao, Z., Zhang, Q., Liu, J. and Dustdar, S. (2024b), "Combining IMU with acoustics for head motion tracking leveraging wireless earphone", *IEEE T. Mobile Comput.*, **23**(6), 6835-6847. <https://doi.org/10.1109/TMC.2023.3325826>
- Hu, J., Jiang, H., Xiao, Z., Chen, S., Dustdar, S. and Liu, J. (2024a), "HeadTrack: Real-time human-computer interaction via wireless earphones", *IEEE J. Sel. Areas Commun.*, **42**(4), 990-1002. <https://doi.org/10.1109/JSAC.2023.3345381>
- Kadoli, R. and Ganesan, N. (2003), "Free vibration and buckling analysis of composite cylindrical shells conveying hot fluid", *Compos. Struct.*, **60**, 19-32. [https://doi.org/10.1016/S0263-8223\(02\)00313-6](https://doi.org/10.1016/S0263-8223(02)00313-6)
- Kong, D., Benabdallah, F. and Kumar, A. (2025), "The effect of smart nanoparticles on the strength and acoustic behaviour in music composition: Theoretical validation", *Adv. Nano Res.*, **18**(2), 163-170. <https://doi.org/10.12989/anr.2025.18.2.163>
- Liew, K.M., Lei, Z.X., Yu, J.L. and Zhang, L.W. (2014), "Postbuckling of carbon nanotube-reinforced functionally graded cylindrical panels under axial compression using a meshless approach", *Comput. Methods Appl. Mech. Engrg.*, **268**, 1-17. <https://doi.org/10.1016/j.cma.2013.09.001>
- Malrin, A., Ducourneau, J. and Chevret, P. (2023), "Characterization and prediction of speech intelligibility at the output of hearing aids in a noisy working environment", *Noise Health*, **25**(118), 183-194. https://doi.org/10.4103/nah.nah_8_23
- Matsuna, H. (2007), "Vibration and buckling of cross-ply laminated composite circular cylindrical shells according to a global higher-order theory", *Int. J. Mech. Sci.*, **49**, 1060-1075. <https://doi.org/10.1016/j.ijmecsci.2006.11.008>
- Merzouki, T. and Houari, M.S.A. (2024a), "Nonlocal strain gradient theory for free vibration analysis of FG nano-scale beams in thermal environments using an efficient numerical model", *J. Vib. Eng. Technol.*, **12**(7), 8775-8800. <https://doi.org/10.1007/s42417-024-01389-x>
- Merzouki, T. and Houari, M.S.A. (2024b), "An efficient numerical model for free vibration of temperature-dependent porous FG nano-scale beams using a nonlocal strain gradient theory", *Struct. Eng. Mech.*, **90**(1), 1-18. <https://doi.org/10.12989/sem.2024.90.1.001>
- Pandey, H.K., Hirwani, C.K., Sharma, N., Katariya, P.V., Dewangan, H.C. and Panda, S.K. (2023), "Effect of nano glass cenosphere filler on hybrid composite eigenfrequency responses—An FEM approach and experimental verification", *Adv. Nano Res.*, **7**(6), 419-429. <http://doi.org/10.12989/anr.2023.7.6.419>
- Seo, Y.S., Jeong, W.B., Yoo, W.S. and Jeong, H.K. (2015), "Frequency response analysis of cylindrical shells conveying fluid using finite element method", *J. Mech. Sci. Technol.*, **19**, 625-633. <https://doi.org/10.1007/BF02916184>
- Sollhoo, S. and Vakis, A.I. (2015), "Single asperity nanocontacts: Comparison between molecular dynamics simulations and continuum mechanics models", *Comput. Mater. Sci.*, **99**, 209-220. <https://doi.org/10.1016/j.commatsci.2014.12.010>
- Tan, P. and Tong, L. (2001), "Micro-electromechanics models for piezoelectric-fiber-reinforced composite materials", *Compos. Sci. Tech.*, **61**, 759-769. [https://doi.org/10.1016/S0266-3538\(01\)00014-8](https://doi.org/10.1016/S0266-3538(01)00014-8)
- Thai, H.T. and Vo, T.P. (2012), "A nonlocal sinusoidal shear deformation beam theory with application to bending, buckling, and vibration of nanobeams", *Int. J. Eng. Sci.*, **54**, 58-66. <https://doi.org/10.1016/j.ijengsci.2012.01.009>
- Wang, T., Hou, B., Li, J., Shi, P., Zhang, B. and Snoussi, H. (2023), "TASTA: Text-assisted spatial and temporal attention network for video question answering", *Adv. Intell. Syst.*, **5**(4), 2200131. <https://doi.org/10.1002/aisy.202200131>
- Wang, S., Yang, R., Li, Z., Jiang, J., Qu, Z., Li, X., and Jiang, C. (2025), "Improvement of pulse compression Rayleigh-wave EMATs. NDT & E International", **155**, 103427. <https://doi.org/10.1016/j.ndteint.2025.103427>
- Wang, T., Li, J., Wu, H., Li, C., Snoussi, H. and Wu, Y. (2022), "ResLNet: deep residual LSTM network with longer input for action recognition", *Front. Comput. Sci.*, **16**(6), 166334. <https://doi.org/10.1007/s11704-021-0236-9>
- Wu, K., Shao, Z., Hong, S. and Qin, S. (2020), "Analytical solutions for mechanical response of circular tunnels with

- double primary linings in squeezing grounds”, *Geomech. Eng.*, **22**(6), 509-518.
<http://doi.org/10.12989/gae.2020.22.6.509>.
- Wuite, J. and Adali, S. (2005), “Deflection and stress behaviour of nanocomposite reinforced beams using a multiscale analysis”, *Compos. Struct.*, **71**, 388-396.
<https://doi.org/10.1016/j.compstruct.2005.09.011>.
- Xie, B., Guo, Y., Chen, Y., Zhang, H., Xiao, J., Hou, M. and Wong, C. (2025), “Advances in graphene-based electrode for triboelectric nanogenerator”, *Nano Micro Lett.*, **17**(1), 17.
<https://doi.org/10.1007/s40820-024-01530-1>
- Xu, B., Wang, X., Zhang, J., Guo, Y. and Razzaqi, A.A. (2022), “A novel adaptive filtering for cooperative localization under compass failure and non-Gaussian noise”, *IEEE T. Veh. Technol.*, **71**(4), 3737-3749.
<https://doi.org/10.1109/TVT.2022.3145095>
- Yang, Y. and Li, H. (2020), “Experimental study on shear behaviors of Partial Precast Steel Reinforced Concrete beams”, *Steel Compos. Struct.*, **37**(5), 605-620,
<http://doi.org/10.12989/scs.2020.37.5.605>
- Zhao, H., Chen, X., Xin, C., Zhao, F., Cheng, S., Lei, M. and Shao, J. (2025a), “High-sensitivity and self-powered flexible pressure sensor based on multi-scale structured piezoelectric composite”, *Chem. Eng. J.*, **519**, 164787.
<https://doi.org/10.1016/j.cej.2025.164787>
- Zhao, K., Wang, H., Wang, X., An, L., Chen, L., Zhang, Y. and Zhou, L. (2025b), “Neutron-gamma discrimination method based on voiceprint identification”, *Radiat. Meas.*, **187**, 107483.
<https://doi.org/10.1016/j.radmeas.2025.107483>
- Zou, H., Alsubih, M., Raja, V.B. and Beemkumar, N. (2025), “Advances in nanoparticle-enhanced music composition based on porous beams: Implications for structural integrity and acoustic performance”, *Adv. Nano Res.*, **18**(1), 75-81.
<https://doi.org/10.12989/anr.2025.18.1.075>.